



Peter Tessier ORCID iD: 0000-0002-3220-007X

Directed evolution of conformation-specific antibodies for sensitive detection of polypeptide aggregates in therapeutic drug formulations

Wenjia Lou^{1,2,†}, Samuel D. Stimple^{1,2,†}, Alec A. Desai², Emily K. Makowski¹, Sibel Kalyoncu⁴, Jesper E. Mogensen⁵, Lotte T. Spang⁵, Désirée J. Asgreen⁵, Arne Staby⁵, Karen Duus⁵, Jan Amstrup⁵, Yulei Zhang², Peter M. Tessier^{1,2,3,4*}

¹Departments of Pharmaceutical Sciences, ²Chemical Engineering, and ³Biomedical Engineering, Biointerfaces Institute, University of Michigan, Ann Arbor, MI 48109, USA

⁴Isermann Department of Chemical & Biological Engineering, Center for Biotechnology & Interdisciplinary Studies, Rensselaer Polytechnic Institute, Troy, NY 12180, USA

⁵Novo Nordisk A/S, Novo Alle 1, DK-2880 Bagsværd, Denmark

Present addresses:

Samuel D. Stimple, Biologics Research, Antibody Discovery, Sanofi US, Framingham, MA 01701

Sibel Kalyoncu, Izmir Biomedicine and Genome Center, Izmir, Turkey

*To whom correspondence should be addressed: Peter M. Tessier

Address: North Campus Research Complex, B10-179

This article has been accepted for publication and undergone full peer review but has not been through the copyediting, typesetting, pagination and proofreading process, which may lead to differences between this version and the Version of Record. Please cite this article as doi: 10.1002/bit.27610.

This article is protected by copyright. All rights reserved.

Accepted Article

2800 Plymouth Road

University of Michigan

Ann Arbor, MI 48109

Email: ptessier@umich.edu

Phone: +1 (734) 763-1486

†Co-first author

Running Title: Polypeptide aggregate immunoassay

Keywords: liraglutide; conformational; amyloid; fibril; aggregation; Thioflavin T

ABSTRACT

Biologics such as peptides and proteins possess a number of attractive attributes that make them particularly valuable as therapeutics, including their high activity, high specificity and low toxicity. However, one of the key challenges associated with this class of drugs is their propensity to aggregate. Given the safety and immunogenicity concerns related to polypeptide aggregates, it is particularly important to sensitively detect aggregates in therapeutic drug formulations as part of the quality control process. Here we report the development of conformation-specific antibodies that recognize polypeptide aggregates composed of a GLP-1 receptor agonist (liraglutide) and their integration into a sensitive immunoassay for detecting liraglutide aggregates. We sorted single-chain antibody libraries against liraglutide aggregates using yeast surface display and magnetic-activated cell sorting, and identified several antibodies with high conformational specificity. Interestingly, these antibodies cross-react with

This article is protected by copyright. All rights reserved.

amyloid fibrils formed by several other polypeptides, revealing that they recognize molecular features common to different types of fibrils. Moreover, we find that our immunoassay using these antibodies is >50-fold more sensitive than the conventional method for detecting liraglutide aggregation (Thioflavin T fluorescence). We expect that our systematic approaches for generating sensitive, aggregate-specific immunoassays can be readily extended to other biologics in order to improve the quality and safety of formulated drug products.

1. INTRODUCTION

Peptide and protein therapeutics are now commonplace in the pharmaceutical industry for treating human disorders ranging from diabetes to cancer (Buss et al., 2012; Elgundi et al., 2017; Lau and Dunn, 2018; A. C. Lee et al., 2019). The many advantages of this class of molecules include those associated with their attractive bioactivity, manufacturability and safety properties (Chiu and Gilliland, 2016; Lau and Dunn, 2018; Starr and Tessier, 2019; Tiller and Tessier, 2015). These unique properties have led to development of diverse therapeutic biomolecules ranging from peptides to antibodies for inhibiting and activating key cellular processes associated with improved health outcomes. Indeed, most of the best-selling drugs today are biologics and the large number of these molecules currently in clinical trials suggests that they will continue to play a prominent role in the therapeutic arena in coming years (Kaplon et al., 2020; Stimple et al., 2019).

Nevertheless, one of the most challenging aspects of developing biologics as drugs is their propensity to form various types of aggregates (C. C. Lee et al., 2013; Lowe et al., 2011; Perchiacca and Tessier, 2012; Redington et al., 2017). This problem is ubiquitous, as all polypeptides display some amount of aggregation if sufficiently stressed. This is particularly concerning because polypeptide aggregates

are multivalent complexes that can elicit immune responses and anti-drug antibodies (De Groot and Scott, 2007; Ratanji et al., 2014; Salazar-Fontana et al., 2017; van Beers et al., 2011). Immunogenicity linked to polypeptide aggregates is one of the leading theories of why some biologics lose their effectiveness after repeated dosing (De Groot and Scott, 2007; Tovey and Lallemand, 2011).

Therefore, it is essential to develop sensitive methods for detecting polypeptide aggregates to improve the development of safe and effective therapeutics. Methods such as size-exclusion chromatography are useful for quantifying soluble aggregates if they are small enough to pass through the column and are present at sufficiently high concentrations (>0.1% or 1000 ppm). However, it is desirable to develop methods that are both orders of magnitude more sensitive for detecting aggregates (<10 ppm) and less dependent on aggregate size. Antibody-based detection assays are well known to be highly sensitive and are attractive for detecting extremely low levels of polypeptide aggregates. However, immunization-based generation of conformation-specific antibodies against polypeptide aggregates is challenging for many reasons, including difficulties in controlling antigen presentation to the immune system, weakly immunogenic antigens in some cases and immunodominant epitopes in other cases, and the fact that most antibodies generated via this process recognize linear (non-conformational) epitopes (Kayed and Glabe, 2006; Lambert et al., 2009; Parray et al., 2020; Vaikath et al., 2019). To address these common challenges, we have used directed evolution methods to generate large antibody libraries and sorted them to isolate conformation-specific antibodies against polypeptide aggregates of a therapeutic GLP-1 agonist (liraglutide) used for treating diabetes and obesity (Croom and McCormack, 2009; Drucker et al., 2010). Moreover, we have characterized and integrated these novel antibodies into a sensitive immunoassay that is able to detect

extremely low levels of liraglutide aggregates in therapeutic peptide formulations (<10 ppm).

2. MATERIALS AND METHODS

2.1 Preparation of liraglutide fibrils

Dry liraglutide polypeptide (Novo Nordisk A/S) was solubilized at a concentration of 6 mg/mL in drug composition buffer (14.0 mg/mL propylene glycol, 5.5 mg/mL phenol, 1.42 mg/mL disodium hydrogen phosphate dihydrate, pH 8.15) and filtered (0.2 μ m filters; 28145-501, VWR International). Liraglutide solution (1 mL) and a 3 mm glass bead were added to a microcentrifuge tube. Fibrils were assembled at 37 °C with agitation (300 rpm, >14 days), and then collected by ultracentrifugation at 221,000 rpm for 1 h at 4 °C (Tube PC Thickwall, 1 mL, 45237, Thermo Fisher Scientific). Fibrils were washed and resuspended in drug composition buffer, and the concentration was determined by BCA assays (23225, Thermo Fisher Scientific). To improve fibril immobilization on magnetic beads and ELISA plates, fibrils were sonicated (FB-120 Sonic Dismembrator, Thermo Fisher Scientific) at 100% amplitude (3 cycles of 10 s on and 30 s off) on ice immediately before the experiments, which reduces fibril size and increases homogeneity.

2.2 Thioflavin T analysis of liraglutide fibrils

Soluble and fibrillated liraglutide samples were separately diluted with drug composition buffer. For fluorescence emission scans, 44.4 μ L of 2.2 μ M Thioflavin T (ThT) was added to 200 μ L of the peptide samples (10 μ M) to achieve a final ThT concentration to 0.4 μ M. The polypeptide/ThT mixtures (50 μ L) were evaluated in black 384-well plates (12566624, Thermo Fisher Scientific). Fluorescence emission scans were performed from 475 to 550 nm (λ_{ex} = 444 nm) at room temperature with a

BioTek Synergy Neo microplate reader. For evaluating the optimal ThT concentration, a range of final ThT concentrations (0.04, 0.4, 4 and 40 μ M) were evaluated.

2.3 Atomic force microscopy of liraglutide fibrils

AFM analysis was performed as described previously (Stimple et al., 2019). Briefly, a 1 \times 1 cm sheet of mica (V- 1 Quality, 71855- 05; Electron Microscopy Sciences, Hatfield, PA) was attached to a glass slide with double-sided tape. Liraglutide fibrils (10 μ L) were then settled on the mica and incubated for 45 min. Next, the sample was washed with sterile water (1 mL) and imaged with an Asylum Research Molecular Force Probe 3D at room temperature. The morphology of the fibrils was determined by tapping- mode (noncontact) imaging in air. The MFP 3D software was used for image processing and analysis of the force data.

2.4 Antibody library preparation, sorting and cloning of selected antibody variants

The antibodies were isolated through two stages of library sorting. In the first stage of sorting, a single-chain variable fragment (scFv) library was generated by diversification of heavy chain CDR3 (HCDR3) of the 4D5 scFv (Julian et al., 2019; Stimple et al., 2019; Tiller, Li, et al., 2017). To avoid concerns related to selection bias towards positively-charged residues (Rabia et al., 2018), the library was diversified at 15 sites in HCDR3, at a frequency of 2-6 amino acids per site, while omitting positively-charged residues (and cysteine) from the library. All members of this library contained a fixed negative charge of HCDR3 (theoretical net charge of -5 at pH 7.4). Under these constraints, at each position the residues sampled were selected on the basis of natural diversity mutagenesis (Tiller, Chowdhury, et al., 2017),

in order to prioritize common residues found in natural antibodies produced by the immune system (Swindells et al., 2017; Tiller, Chowdhury, et al., 2017).

The diversified scFvs (theoretical library diversity of 3.6×10^7) were cloned in yeast (EBY100) via homologous recombination into a yeast surface display vector as C-terminal fusions to the yeast mating protein Aga2. The yeast display vector was a closely related derivative of pCTCON2 containing a modified linker between Aga2 and the scFvs (Julian et al., 2019). Yeast harboring the plasmids were cultured, propagated, and recovered after sorting in low-pH SDCAA medium (20 g dextrose, 5 g casamino acids, 6.7 g yeast nitrogen base without amino acids, 16.75 g sodium citrate and 4 g anhydrous citric acid per liter) with shaking at 30 °C. Yeast surface display of the scFvs was induced by transferring the cultures at the mid-exponential phase of growth (OD_{600} of 2-4) into SGCAA medium (20 g galactose, 5 g casamino acids, 6.7 g yeast nitrogen base without amino acids, 8.56 g sodium dihydrogen phosphate monohydrate and 5.4 g sodium phosphate dibasic per liter) and culturing with shaking at 30 °C for 20 h prior to sorting.

Yeast-displayed antibody libraries were sorted for binding to liraglutide fibrils immobilized on magnetic beads (Dynabeads M-280 Tosylactivated, 14203, Invitrogen) via the N-terminal amine of liraglutide. To prepare the beads, 8×10^7 beads were first washed (2x) with 1 mL of sterile PBS. Soluble liraglutide (100 µg obtained from a 6 mg/mL stock in drug composition buffer) was diluted into PBS containing the magnetic beads (final volume of 800 µL) and coupled to the beads overnight (4 °C without agitation). For beads coated with fibrillar liraglutide, fibrils (100 µg) were coupled to the beads in PBS (800 µL) overnight at room temperature with end-over-end mixing. The following day, the beads were washed twice with 1 mL PBS supplemented with 10 mM glycine in order to quench unreacted Tosyl groups on the

beads, and then washed twice using 1 mL of PBS supplemented with 1 g/L BSA (PBS-B) before incubation with yeast. Eight rounds of positive selections were performed against beads coated with liraglutide fibrils in PBS-B supplemented with 1 % milk. In order to isolate yeast harboring conformation-specific antibodies against liraglutide fibrils, the final three rounds of sorting incorporated negative selections performed against beads coated with soluble liraglutide in PBS-B prior to the positive selection against liraglutide fibrils.

In the second stage of library sorting (affinity maturation), a sub-library was designed for one of the best clones from the first stage of sorting. The second-generation library contained diversified sites in light chain CDR1 (LCDR1), LCDR3 and HCDR2. This library was diversified at eleven sites in LCDR1, LCDR3, and HCDR2 of clone LA at a frequency of 4-6 amino acids per site, yielding a theoretical library size of 1.1×10^8 . The sites chosen for diversification were selected based on a variety of criteria. First, aspartic acid (D) and tyrosine (Y) were prioritized in the diversification scheme. The sites that were mutated all met one of three criteria: 1) sites where D and Y are observed in human antibodies at a frequency of 2% or higher and the wild-type residue in clone (LA) is D, Y, A, S, G, C, V, or F; 2) sites where D or Y are observed in human antibodies at a frequency of 2% or higher and the wild-type residue in clone LA is D, Y, A, S, G, C, V, or F; 3) sites where D or Y are observed in human antibodies at a frequency of 2% or higher and the wild-type residue in clone LA is I, T, or N. When all CDR sites (excluding those in the previously evolved HCDR3) meeting any of these criteria had been identified, they were ranked from most diverse to least diverse in human antibodies, using the frequency of the most-commonly observed residue in nature as a metric for diversity. The eleven most diverse sites were selected, and 4-6 residues were sampled at each

position. Stop codons and positively-charged residues were omitted from the library design, and the inclusion of D and/or Y, as well as the wild-type residue, was forced at each diversification site. The additional residues that were sampled at each site were selected in order to maximize coverage of human antibody diversity. The library was synthesized through an overlap PCR procedure utilizing degenerate primers encoding the diversity sampled in each CDR, and the library was transformed into yeast via electroporation and homologous recombination, as described above.

This library was subjected to four rounds of selection against liraglutide fibrils. The first two rounds of sorting each incorporated two sequential negative selections against soluble liraglutide (immobilized on magnetic beads) prior to a positive selection against immobilized liraglutide fibrils. Negative selections were performed in PBS-B, while positive selections were conducted in PBS-B supplemented with 1% milk. Three sequential negative selections in rounds 3 and 4 were also performed against beads coated with glucagon fibrils. The beads coated with glucagon fibrils were prepared as previously described (Stimple et al., 2019).

The selected antibodies were cloned into the mammalian expression vector anti-Notch1_E6-pBIOCAM5, as described previously (Stimple et al., 2019). Briefly, the insert and the backbone plasmids were digested with *NcoI*-HF and *NotI*-HF, purified and ligated. The insertion of the scFv coding fragments was confirmed by Sanger sequencing. These plasmids express a bivalent scFv-human Fc fusion protein with 6xHis and 3xFLAG tags on their C-terminus.

2.5 Antibody expression and purification

Proteins were expressed with the Expi293 Expression System (A14635, Invitrogen). Expi293F cells were subcultured and expanded until the cells reached a

density of approximately 3-5 million viable cells per mL. Complexes of ExpiFectamine 293 and plasmid DNA (30 µg per 25 mL of culture) were prepared as described in the manufacturer's protocol. Briefly, plasmid DNA and ExpiFectamine reagent were diluted separately in Opti-MEM medium and mixed via gentle pipetting. After 5 min of incubation, the diluted transfection reagent was mixed with the diluted DNA. The complexes of transfection reagent and DNA were incubated at room temperature for 20 min and added to the Expi293F cells. Cells were incubated at 37 °C and 5% CO₂ with shaking. Per the manufacturer's instructions, enhancer 1 and 2 solutions were added to the cells after 20 h (post transfection). After 3 d, the media containing secreted antibody was harvested and centrifuged at 3400 xg for 45 min to remove the cells and associated debris.

Antibodies were purified using Protein A chromatography. Protein A beads (20334, Thermo Fisher Scientific) were washed with PBS and then 0.5 mL of beads were added to 30 mL of clarified media and incubated 4 °C with gentle rocking. On the following day, media with Protein A beads was added to a 10 mL purification column (89898, Thermo Fisher Scientific). The beads were collected through vacuum filtration and washed thoroughly with PBS (100 mL). The Protein A beads were then incubated with 2 mL of 0.1 M glycine buffer (pH 3.0) for 15 min and the buffer (with eluted protein) was collected by centrifugation. The eluted antibodies were then buffer exchanged into PBS using Zeba Spin Desalting Columns (89891, Thermo Fisher Scientific). Protein concentrations were assayed via absorbance measurements at 280 nm (extinction coefficients of 149,800-173,100 M⁻¹ cm⁻¹).

2.6 Size-exclusion chromatography

Analytical and preparative size-exclusion chromatography (SEC) experiments were performed using a Shimadzu Prominence HPLC System. The running buffer

was 137 mM sodium chloride, 2.7 mM sodium-potassium, 10 mM disodium hydrogen phosphate, 1.8 mM potassium dihydrogen phosphate and 200 mM arginine (pH 7.4). The column flow rate was 0.75 mL/min. The antibody samples (0.1 mg/mL) were injected (100 μ L) into the column (GE 28990944, Superdex 200 Increase 10/300 GL column), and absorbance signals were monitored at 220 and 280 nm. For preparative SEC, the monomeric fraction was isolated using an FRC-10A fraction collector based on time points determined from analytical experiments.

2.7 Antibody stability analysis

Antibody (LA-5) samples were diluted to 0.1 mg/mL in PBS (pH 7.4) and aliquoted (120 μ L/tube). Six samples (tubes) were prepared for each group. The control group was kept at 4 °C. One group was incubated at 25 °C without shaking. The freeze-thaw samples were treated by freezing at -80 °C overnight and thawing at room temperature five times. After 7 d, the samples were analyzed by SEC. Three independent experiments were performed (two replicates per experiment).

2.7 Immunoassay

2.7.1 Initial antibody binding analysis

Nunc MaxiSorp 96-well ELISA plates (439454, Thermo Fisher Scientific) were incubated with 150 μ L of BSA (1 mg/mL) in PBS overnight at 4 °C, as reported previously to maximize sensitivity (Stimple et al., 2019). On the day of assay, the BSA solution was removed and soluble and fibrillar liraglutide solutions (100 μ L of 10 μ M liraglutide) were incubated at room temperature for 3 h. The well plates were then washed three times with PBS. The specificity of each two-step purified antibody was determined by incubating the immobilized antigens with various concentrations of antibody in PBST (PBS with 0.1% Tween 20) supplemented with 1 mg/mL BSA

for 1 h. The well plates were washed three times with PBST. Next, secondary antibody (Goat anti-Human IgG Fc HRP-conjugate, A18817, Thermo Fisher Scientific) was diluted 1:1000 (stock concentration of 0.5 mg/mL) in PBST supplemented with 10 mg/mL BSA and added to the well plates (100 μ L) for 1 h. The well plates were washed three times and then substrate (100 μ L 1-Step Ultra-TMB ELISA Substrate Solution; 34028, Thermo Fisher Scientific) was added. After incubation for 5 min, the reaction was quenched with 100 μ L of 2 M sulfuric acid. Secondary antibody binding was determined by measuring the absorbance at 450 nm using a Biotek Synergy Neo microplate reader. The reported values represent the binding signals for fibrils relative to soluble peptide or background.

2.7.2 Immunoassay detection of liraglutide fibrils in mixtures of soluble and aggregated peptide

ELISA plates were coated with BSA as described above. On the day of the assay, liraglutide fibrils were diluted with soluble liraglutide to concentrations ranging from 0.001 to 250 μ M while maintaining a total liraglutide concentration at 1600 μ M. Next, the samples were incubated in plates blocked with BSA (1 mg/mL) for 3 h at room temperature. The plates were washed (PBS), and fibrils were detected using primary antibodies (100 nM) in PBST with BSA (0, 0.1, 1 and 10 mg/mL). Next, the bound primary antibodies were detected with the appropriate secondary HRP-conjugated antibodies and substrates, as described above. Experiments were also performed using primary antibodies (100, 50 and 25 nM) diluted with PBST in the absence of BSA.

2.7.3 Evaluation of antibody binding specificity using different types of amyloid fibrils

α -synuclein fibrils (145 μ M) were assembled at 37 $^{\circ}$ C in 20 mM HEPES, 100 mM NaCl and 1 mM EDTA (pH 7.4) with shaking (1000 rpm for 3 d). Glucagon fibrils (287 μ M) were assembled at 37 $^{\circ}$ C with shaking (900 rpm for 18 h), as described

previously (Stimple et al., 2019). All fibrils were purified via sedimentation (221,000xg for 1 h at 4 °C). Fibril antigens were immobilized in non-treated Nunc MaxiSorp 96-well ELISA plates overnight at 4 °C. Antibody binding (LA-5) was evaluated at 50 nM (PBST), as described above.

2.7.4 Immunoblot analysis of liraglutide antibody conformational specificity

Soluble and fibrillar glucagon and liraglutide were immobilized on nitrocellulose membranes (10600004, Amersham Protran, GE Healthcare) at a range of concentrations and allowed to dry to room temperature for at least 2 h. The blots were then blocked with 5% milk in PBS at room temperature for 1 h followed by washing (3x) with PBST and mild agitation for 5 min each. Next, the blots were incubated with antibody (50 nM) in PBST at room temperature for 1-2 h followed by washing (3x) with PBST and incubation with goat anti-human IgG Fc-HRP conjugate (1/5000x dilution) at room temperature for 1 h. Finally, the blots were washed with PBST (3x), developed with ECL (32106, Invitrogen), and imaged using Biorad Chemidoc XRS imager.

3. RESULTS

3.1 Identification and characterization of antibodies specific for liraglutide fibrils

To generate conformational antibodies against liraglutide fibrils, we first prepared soluble and aggregated forms of liraglutide. Toward this end, we assembled liraglutide fibrils in its formulation buffer (6 mg/mL peptide at pH 8.15 with propylene glycol, phenol and phosphate). We found that a moderate agitation rate (300 rpm with a glass bead) at 37 °C for two weeks was effective at promoting fibril formation. Aggregates that were purified using high speed centrifugation (221,000xg) were strongly positive for the amyloid-specific dye Thioflavin T (Fig. 1A). Moreover,

we found that the liraglutide aggregates were fibrillar in structure using AFM imaging (Fig. 1B).

We next immobilized the liraglutide fibrils on magnetic beads and sorted single-chain (scFv) antibody libraries displayed on the surface of yeast using magnetic-activated cell sorting. After multiple rounds of sorting, we sequenced 30 clones from the final enriched library and identified 16 unique variants. We evaluated 12 of these clones as Fc fusion proteins in more detail. Our attempts to express them in suspension HEK293 cells and purify them via Protein A chromatography resulted in variable purification yields. Five of the 12 antibodies were purified at yields <20 mg/L and were excluded from further analysis (Fig. 2A). However, the remaining seven antibodies were subjected to a second step purification step using size-exclusion chromatography. While all seven antibodies were successfully purified via size-exclusion chromatography, three of the antibodies (LA-2, LA-5 and LA-7) were two-step purified at yields >20 mg/L. The purified antibodies were predominantly monomeric, as demonstrated by analytical size-exclusion chromatography (>95% monomer for LA-2, LA-5 and LA-7; Fig. 2B).

To initially evaluate the binding activity of the antibodies, we tested their recognition of liraglutide fibrils relative to soluble liraglutide (Figs. 3 and S1). The antibodies at low concentrations (5 nM) displayed normalized binding signals that were two- to six-fold greater for liraglutide fibrils than soluble liraglutide and blank wells (no immobilized peptide; Fig. 3), and which was generally enhanced relative to the parental antibody (LA; Fig. S1). The fact that the antibodies displayed similar binding to soluble liraglutide and blank wells suggested low non-specific binding. We also characterized the best binding antibody (LA-5) in terms of its concentration-dependent binding to fibrillar and soluble liraglutide relative to the parental (LA) and

wild-type (WT) antibodies (Fig. 4). Importantly, LA-5 displayed significantly improved selective binding to liraglutide fibrils relative to the parental and wild-type antibodies. The EC_{50} value for LA-5 binding to liraglutide fibrils was 30 ± 2 nM. These results confirm that LA-5 displays strong conformational specificity for liraglutide fibrils.

3.2 Evaluation of ELISA detection selectivity and sensitivity

We next sought to further improve the selectivity and sensitivity of our best antibody (LA-5) for detecting liraglutide fibrils (Fig. 5). Our initial experiments used BSA (1 mg/mL) during the primary antibody binding step to block non-specific interactions. However, we suspected that non-specific interactions were not a significant problem and that antibody sensitivity could be improved by reducing the BSA concentration. To evaluate this, we performed the detection experiments using mixtures of fibrillar and soluble liraglutide peptide to simulate detection of fibrils (0.001-30 μ M) in liraglutide formulations (1600 μ M). Notably, we found that reducing (0.1 mg/mL) or eliminating BSA led to significant improvements in selective antibody binding to liraglutide fibrils (Fig. 5A). For example, removing BSA led to selective antibody binding (>3-fold greater binding to samples with fibrils and soluble peptide relative to those with only soluble peptide) at fibril concentrations as low as 0.01 μ M (relative to 1600 μ M soluble peptide), which corresponds to detection of 6 ppm fibrils. Moreover, we found that the optimal antibody concentration for detecting liraglutide fibrils was 50 nM, which led to modestly improved binding signals relative to lower (25 nM) and higher (100 nM) antibody concentrations (Fig. 5B).

We also evaluated the specificity of LA-5 for recognizing liraglutide fibrils relative to fibrils formed from other amyloidogenic polypeptides (Fig. 6). Given previous reports of other amyloid-specific antibodies cross-reacting with diverse types of amyloid fibrils (Kayed et al., 2007; O'Nuallain and Wetzel, 2002; Stimple et al., 2019), we sought to test if LA-5 recognized an epitope specific to liraglutide fibrils or a sequence-independent features common to diverse types of amyloid fibrils. Indeed, we found that LA-5 cross-reacted with glucagon and α -synuclein fibrils, while failing to recognize soluble forms of both polypeptides. Moreover, LA-5 also recognized IAPP and A β fibrils (data not shown). These findings confirm that the binding mechanism of LA-5 involves molecular features common to multiple types of amyloid fibrils.

We also sought to evaluate if the conformational specificity of LA-5 was specific to the ELISA format or if it was more generally observed in different assay formats such as immunoblots (Fig. 7). Therefore, we deposited soluble and aggregated liraglutide and glucagon on nitrocellulose membranes and probed with LA-5. Notably, we observed strict conformational specificity of LA-5 for liraglutide fibrils relative to soluble peptide. Moreover, we also observed reactivity of LA-5 with aggregated but not soluble glucagon, confirming that the antibody cross reacts with molecular features common in different types of in amyloid fibrils.

Next, we sought to compare the sensitivity of our improved ELISA assay to the conventional method of detecting fibrils in liraglutide formulations, namely ThT fluorescence (Fig. 8). We first evaluated the most sensitive concentration of ThT for detection of fibrils in the presence of high concentrations of soluble liraglutide (1600 μ M; Fig. S1). Interestingly, we found that a relatively low ThT concentration (0.4 μ M) is optimal, while higher (4-40 μ M) and lower (0.04 μ M) concentrations led to

This article is protected by copyright. All rights reserved.

reduced signal. At 0.4 μM ThT, the detection limit (>3 -fold greater binding to fibrils relative to soluble peptide) is 0.19 μM liraglutide fibrils. Importantly, the detection sensitivity of LA-5 at the same conditions is greatly improved, as the detection limit is 0.0036 μM or >50 -fold lower than ThT.

Finally, we evaluated the stability of LA-5 to determine if it possesses the necessary properties for reliable and reproducible use in ELISAs for detection of liraglutide fibrils (Fig. 9). This was particularly important because LA-5 possessed ~ 30 - 35% aggregate after Protein A purification (data not shown), and a second step purification was required to reduce the aggregate to $<5\%$. We tested if the purified antibody would aggregate simply by storing it at room temperature for one week or repeatedly freezing and thawing it (five times). Encouragingly, we find that neither condition induced aggregation ($<5\%$ aggregate), suggesting that the antibody is sufficiently stable for repeated use in assays for detecting liraglutide aggregates.

4. DISCUSSION

The significance of our findings related to development of a sensitive immunoassay for detecting liraglutide fibrils deserves further consideration. It is well known that ThT assays – which are the gold standard for detecting liraglutide fibrils at low concentrations (e.g., <1000 ppm) – yield variable results that are difficult to reproduce. One reason for this lack of reproducibility is that agitation is often used to amplify pre-existing fibrils via seeding to increase the fibril concentration and enhance detection. However, a drawback of this approach is the variability of the agitation-induced seeding process that often requires extended periods of time (e.g., many hours to days). In this work, we excluded agitation from the ELISA and ThT assays, and performed the experiments over relatively short periods of time (e.g.,

hours) to increase reproducibility. Indeed, we find our sensitive ELISA is highly reproducible for detecting pre-existing aggregates without the need to first amplify aggregates through agitation-induced seeding. Such fibrillization assays may be essential for robust evaluation of the quality of liraglutide products and to ensure their safety for patients (Staby et al., 2020).

The conformational antibodies reported in this work against liraglutide fibrils and related conformational antibodies against glucagon fibrils (Stimple et al., 2019), which were produced using similar directed evolution methods, possess several unique molecular features relative to other conformational and conventional antibodies. First, the heavy chain CDR3s of our liraglutide and glucagon antibodies have unusually large numbers of aromatic amino acids (10.3 ± 1.4 Trp, Phe and Tyr residues) relative to A β conformational (2.9 ± 1.9 aromatic residues) and non-conformational (2.6 ± 2.1 aromatic residues) antibodies [see (Julian et al., 2019) for a summary of these antibodies] as well as human antibodies in general (3.3 ± 1.7 aromatic residues). Second, our liraglutide and glucagon conformational antibodies have heavy chain CDR3s that are much more negatively charged (-5.8 ± 0.4 net charge at pH 7.4) than those of A β conformational (-0.3 ± 1.6) and non-conformational (-1.4 ± 1.5) antibodies as well as human antibodies in general (-1.4 ± 1.3). We speculate that the unique combination of these two properties may be important in balancing antibody affinity and specificity. This hypothesis is based on the observations that various types of aromatic residues and moieties are known to be key determinants of amyloid formation and to interact with amyloid fibrils (Chen et al., 2020; Frydman-Marom et al., 2011; Ladiwala et al., 2011; Levy-Sakin et al., 2009; Stains et al., 2007), and negatively-charged residues are known to increase antibody specificity and reduce non-specific binding (Li et al., 2014; Rabia et al., 2018; Sakhnini et al., 2019;

Schaefer et al., 2016; Starr and Tessier, 2019; Zhang et al., 2020), including for conformational antibodies (Julian et al., 2019; C. C. Lee et al., 2016; Rabia et al., 2018).

There are multiple aspects of our assay that also deserve further consideration. First, we found that it was critical for the reproducibility of our assay to perform a two-step purification (Protein A and size-exclusion chromatography) to remove antibody aggregates introduced upon low pH elution from the Protein A resin. Our initial experiments that employed one-step purified antibodies revealed that antibody aggregates bound to liraglutide aggregates, which resulted in both variable antibody reactivity and assay performance between different batches of purified antibody. After removing antibody aggregates using size-exclusion chromatography, we found that the assay reproducibility was significantly improved, including for results obtained using different batches of purified antibody. Second, we found that relatively high antibody concentrations (50 nM) were optimal for liraglutide fibril detection. Interestingly, our antibodies displayed low levels of non-specific interactions at relatively high antibody concentrations (up to 100 nM). It is relatively common for antibodies to display non-specific interactions at such high concentrations (Jain et al., 2017; Rabia et al., 2018), and the lack of such non-specific interactions likely explains (at least in part) the excellent performance of our antibodies.

There are also several outstanding questions that will need to be addressed in future work. First, it will be important to evaluate if our antibodies recognize liraglutide aggregates – such as non-fibrillar aggregates – that are not recognized by ThT. Amyloid-forming peptides like liraglutide form a number of different types of prefibrillar oligomers and fibrillar aggregates (Chiti and Dobson, 2006; Dobson, 2003; Glabe, 2008), some of which are not recognized by ThT (Glabe, 2008; Quittot

et al., 2018; Wu et al., 2010). If our antibodies detect such non-ThT positive aggregates or can be further evolved to do so, this would increase their utility and importance. Second, it will be important to evaluate if our sensitive immunoassay can be used to detect differences in levels of endogenous aggregates that form in different batches of formulated liraglutide. In this work, we doped liraglutide formulations with different levels of preformed liraglutide fibrils. It will be important in the future to evaluate if these findings can be translated to detecting low levels of endogenous aggregates that may form during manufacturing and/or processing steps. In particular, it will be crucial to evaluate if antibody detection of low initial levels of fibrils at the drug release stage can be used to predict the levels of fibrils that form slowly during years of storage.

5. CONCLUSIONS

We report a robust and reproducible ELISA using novel conformational antibodies for sensitively detecting liraglutide aggregates at extremely low concentrations (<10 ppm). The strengths of the assay are related to its simplicity, the ability to detect aggregates in a manner weakly dependent on aggregate size, and the lack of need for agitation and amplification of pre-existing aggregates. The latter issue has plagued sensitive Thioflavin T assays and often results in poor assay reproducibility. More generally, we expect that the methods reported in this work can be readily applied to generate sensitive ELISAs for detecting aggregates formed by diverse amyloid-forming peptides and proteins.

ACKNOWLEDGMENTS

We thank members of the Tessier lab for their helpful suggestions. This work was supported by Novo Nordisk A/S, and the Albert M. Mattocks Chair (to P.M.T).

CONFLICTS OF INTEREST

J.E.M., L.T.S., D.J.A., A.S., K.D. and J.A. are employees of Novo Nordisk A/S. P.M.T. has received an honorarium and consulting fees from Novo Nordisk A/S.

AUTHOR CONTRIBUTIONS

W.L., S.D.S., A.A.D., E.K.M., S.K., J.E.G., A.S. and P.M.T. designed the research, S.D.S. and A.A.D. constructed the antibody libraries and performed the antibody sorting. S.D.S., W.L., and E.K.M. performed the characterization of antibodies. S.K. performed the atomic force microscopy of liraglutide fibrils. Y.Z. performed antibody sequence and bioinformatics analysis. W.L., S.D.S., A.A.D., E.K.M., J.E.G., L.T.S., D.J.A., A.S., K.D., J.A and P.M.T. analyzed the data. W.L., S.D.S., A.A.D. and P.M.T. wrote the paper with input from the co-authors.

REFERENCES

- Buss, N. A., Henderson, S. J., McFarlane, M., Shenton, J. M., & de Haan, L. (2012). Monoclonal antibody therapeutics: history and future. *Curr Opin Pharmacol*, 12(5), 615-622. doi:10.1016/j.coph.2012.08.001
- Chen, Y., Wei, G., Zhao, J., Nussinov, R., & Ma, B. (2020). Computational Investigation of Gantenerumab and Crenezumab's Recognition of Abeta Fibrils in Alzheimer's Disease Brain Tissue. *ACS Chem Neurosci*. doi:10.1021/acscchemneuro.0c00364
- Chiti, F., & Dobson, C. M. (2006). Protein misfolding, functional amyloid, and human disease. *Annu Rev Biochem*, 75, 333-366. doi:10.1146/annurev.biochem.75.101304.123901
- Chiu, M. L., & Gilliland, G. L. (2016). Engineering antibody therapeutics. *Curr Opin Struct Biol*, 38, 163-173. doi:10.1016/j.sbi.2016.07.012
- Croom, K. F., & McCormack, P. L. (2009). Liraglutide: a review of its use in type 2 diabetes mellitus. *Drugs*, 69(14), 1985-2004. doi:10.2165/11201060-000000000-00000
- De Groot, A. S., & Scott, D. W. (2007). Immunogenicity of protein therapeutics. *Trends Immunol*, 28(11), 482-490. doi:10.1016/j.it.2007.07.011

- Dobson, C. M. (2003). Protein folding and misfolding. *Nature*, 426(6968), 884-890. doi:10.1038/nature02261
- Drucker, D. J., Dritselis, A., & Kirkpatrick, P. (2010). Liraglutide. *Nat Rev Drug Discov*, 9(4), 267-268. doi:10.1038/nrd3148
- Elgundi, Z., Reslan, M., Cruz, E., Sifniotis, V., & Kayser, V. (2017). The state-of-play and future of antibody therapeutics. *Adv Drug Deliv Rev*, 122, 2-19. doi:10.1016/j.addr.2016.11.004
- Frydman-Marom, A., Shaltiel-Karyo, R., Moshe, S., & Gazit, E. (2011). The generic amyloid formation inhibition effect of a designed small aromatic beta-breaking peptide. *Amyloid*, 18(3), 119-127. doi:10.3109/13506129.2011.582902
- Glabe, C. G. (2008). Structural classification of toxic amyloid oligomers. *J Biol Chem*, 283(44), 29639-29643. doi:10.1074/jbc.R800016200
- Jain, T., Sun, T., Durand, S., Hall, A., Houston, N. R., Nett, J. H.,... Witttrup, K. D. (2017). Biophysical properties of the clinical-stage antibody landscape. *Proc Natl Acad Sci U S A*, 114(5), 944-949. doi:10.1073/pnas.1616408114
- Julian, M. C., Rabia, L. A., Desai, A. A., Arsiwala, A., Gerson, J. E., Paulson, H. L.,... Tessier, P. M. (2019). Nature-inspired design and evolution of anti-amyloid antibodies. *J Biol Chem*, 294(21), 8438-8451. doi:10.1074/jbc.RA118.004731
- Kaplon, H., Muralidharan, M., Schneider, Z., & Reichert, J. M. (2020). Antibodies to watch in 2020. *MAbs*, 12(1), 1703531. doi:10.1080/19420862.2019.1703531
- Kayed, R., & Glabe, C. G. (2006). Conformation-dependent anti-amyloid oligomer antibodies. *Methods Enzymol*, 413, 326-344. doi:10.1016/S0076-6879(06)13017-7
- Kayed, R., Head, E., Sarsoza, F., Saing, T., Cotman, C. W., Neuclea, M.,... Glabe, C. G. (2007). Fibril specific, conformation dependent antibodies recognize a generic epitope common to amyloid fibrils and fibrillar oligomers that is absent in prefibrillar oligomers. *Mol Neurodegener*, 2, 18. doi:10.1186/1750-1326-2-18
- Ladiwala, A. R., Dordick, J. S., & Tessier, P. M. (2011). Aromatic small molecules remodel toxic soluble oligomers of amyloid beta through three independent pathways. *J Biol Chem*, 286(5), 3209-3218. doi:10.1074/jbc.M110.173856
- Lambert, M. P., Velasco, P. T., Viola, K. L., & Klein, W. L. (2009). Targeting generation of antibodies specific to conformational epitopes of amyloid beta-derived neurotoxins. *CNS Neurol Disord Drug Targets*, 8(1), 65-81. doi:10.2174/187152709787601876
- Lau, J. L., & Dunn, M. K. (2018). Therapeutic peptides: Historical perspectives, current development trends, and future directions. *Bioorg Med Chem*, 26(10), 2700-2707. doi:10.1016/j.bmc.2017.06.052

- Lee, A. C., Harris, J. L., Khanna, K. K., & Hong, J. H. (2019). A Comprehensive Review on Current Advances in Peptide Drug Development and Design. *Int J Mol Sci*, 20(10). doi:10.3390/ijms20102383
- Lee, C. C., Julian, M. C., Tiller, K. E., Meng, F., DuConge, S. E., Akter, R.,... Tessier, P. M. (2016). Design and Optimization of Anti-amyloid Domain Antibodies Specific for beta-Amyloid and Islet Amyloid Polypeptide. *J Biol Chem*, 291(6), 2858-2873. doi:10.1074/jbc.M115.682336
- Lee, C. C., Perchiacca, J. M., & Tessier, P. M. (2013). Toward aggregation-resistant antibodies by design. *Trends Biotechnol*, 31(11), 612-620. doi:10.1016/j.tibtech.2013.07.002
- Levy-Sakin, M., Shreberk, M., Daniel, Y., & Gazit, E. (2009). Targeting insulin amyloid assembly by small aromatic molecules: toward rational design of aggregation inhibitors. *Islets*, 1(3), 210-215. doi:10.4161/isl.1.3.9609
- Li, B., Tesar, D., Boswell, C. A., Cahaya, H. S., Wong, A., Zhang, J.,... Kelley, R. F. (2014). Framework selection can influence pharmacokinetics of a humanized therapeutic antibody through differences in molecule charge. *MAbs*, 6(5), 1255-1264. doi:10.4161/mabs.29809
- Lowe, D., Dudgeon, K., Rouet, R., Schofield, P., Jermutus, L., & Christ, D. (2011). Aggregation, stability, and formulation of human antibody therapeutics. *Adv Protein Chem Struct Biol*, 84, 41-61. doi:10.1016/B978-0-12-386483-3.00004-5
- O'Nuallain, B., & Wetzel, R. (2002). Conformational Abs recognizing a generic amyloid fibril epitope. *Proc Natl Acad Sci U S A*, 99(3), 1485-1490. doi:10.1073/pnas.022662599
- Parray, H. A., Shukla, S., Samal, S., Shrivastava, T., Ahmed, S., Sharma, C., & Kumar, R. (2020). Hybridoma technology a versatile method for isolation of monoclonal antibodies, its applicability across species, limitations, advancement and future perspectives. *Int Immunopharmacol*, 85, 106639. doi:10.1016/j.intimp.2020.106639
- Perchiacca, J. M., & Tessier, P. M. (2012). Engineering aggregation-resistant antibodies. *Annu Rev Chem Biomol Eng*, 3, 263-286. doi:10.1146/annurev-chembioeng-062011-081052
- Quittot, N., Sebastiao, M., Al-Halifa, S., & Bourgault, S. (2018). Kinetic and Conformational Insights into Islet Amyloid Polypeptide Self-Assembly Using a Biarsenical Fluorogenic Probe. *Bioconjugate Chemistry*, 29(2), 517-527. doi:10.1021/acs.bioconjchem.7b00827
- Rabia, L. A., Zhang, Y., Ludwig, S. D., Julian, M. C., & Tessier, P. M. (2018). Net charge of antibody complementarity-determining regions is a key predictor of specificity. *Protein Eng Des Sel*, 31(11), 409-418. doi:10.1093/protein/gzz002

- Ratanji, K. D., Derrick, J. P., Dearman, R. J., & Kimber, I. (2014). Immunogenicity of therapeutic proteins: influence of aggregation. *J Immunotoxicol*, *11*(2), 99-109. doi:10.3109/1547691X.2013.821564
- Redington, J. M., Breydo, L., & Uversky, V. N. (2017). When Good Goes Awry: The Aggregation of Protein Therapeutics. *Protein Pept Lett*, *24*(4), 340-347. doi:10.2174/0929866524666170209153421
- Sakhnini, L. I., Greisen, P. J., Wiberg, C., Bozoky, Z., Lund, S., Wolf Perez, A. M.,... Pedersen, A. K. (2019). Improving the Developability of an Antigen Binding Fragment by Aspartate Substitutions. *Biochemistry*, *58*(24), 2750-2759. doi:10.1021/acs.biochem.9b00251
- Salazar-Fontana, L. I., Desai, D. D., Khan, T. A., Pillutla, R. C., Prior, S., Ramakrishnan, R.,... Joseph, A. (2017). Approaches to Mitigate the Unwanted Immunogenicity of Therapeutic Proteins during Drug Development. *AAPS J*, *19*(2), 377-385. doi:10.1208/s12248-016-0030-z
- Schaefer, Z. P., Bailey, L. J., & Kossiakoff, A. A. (2016). A polar ring endows improved specificity to an antibody fragment. *Protein Sci*, *25*(7), 1290-1298. doi:10.1002/pro.2888
- Stains, C. I., Mondal, K., & Ghosh, I. (2007). Molecules that target beta-amyloid. *ChemMedChem*, *2*(12), 1674-1692. doi:10.1002/cmdc.200700140
- Starr, C. G., & Tessier, P. M. (2019). Selecting and engineering monoclonal antibodies with drug-like specificity. *Curr Opin Biotechnol*, *60*, 119-127. doi:10.1016/j.copbio.2019.01.008
- Stimple, S. D., Kalyoncu, S., Desai, A. A., Mogensen, J. E., Spang, L. T., Asgreen, D. J.,... Tessier, P. M. (2019). Sensitive detection of glucagon aggregation using amyloid fibril-specific antibodies. *Biotechnol Bioeng*, *116*(8), 1868-1877. doi:10.1002/bit.26994
- Swindells, M. B., Porter, C. T., Couch, M., Hurst, J., Abhinandan, K. R., Nielsen, J. H.,... Martin, A. C. (2017). abYsis: Integrated Antibody Sequence and Structure-Management, Analysis, and Prediction. *J Mol Biol*, *429*(3), 356-364. doi:10.1016/j.jmb.2016.08.019
- Tiller, K. E., Chowdhury, R., Li, T., Ludwig, S. D., Sen, S., Maranas, C. D., & Tessier, P. M. (2017). Facile Affinity Maturation of Antibody Variable Domains Using Natural Diversity Mutagenesis. *Front Immunol*, *8*, 986. doi:10.3389/fimmu.2017.00986
- Tiller, K. E., Li, L., Kumar, S., Julian, M. C., Garde, S., & Tessier, P. M. (2017). Arginine mutations in antibody complementarity-determining regions display context-dependent affinity/specificity trade-offs. *J Biol Chem*, *292*(40), 16638-16652. doi:10.1074/jbc.M117.783837
- Tiller, K. E., & Tessier, P. M. (2015). Advances in Antibody Design. *Annu Rev Biomed Eng*, *17*, 191-216. doi:10.1146/annurev-bioeng-071114-040733

- Tovey, M. G., & Lallemand, C. (2011). Immunogenicity and other problems associated with the use of biopharmaceuticals. *Ther Adv Drug Saf*, 2(3), 113-128. doi:10.1177/2042098611406318
- Vaikath, N. N., Hmila, I., Gupta, V., Erskine, D., Ingelsson, M., & El-Agnaf, O. M. A. (2019). Antibodies against alpha-synuclein: tools and therapies. *J Neurochem*, 150(5), 612-625. doi:10.1111/jnc.14713
- van Beers, M. M., Sauerborn, M., Gilli, F., Brinks, V., Schellekens, H., & Jiskoot, W. (2011). Oxidized and aggregated recombinant human interferon beta is immunogenic in human interferon beta transgenic mice. *Pharm Res*, 28(10), 2393-2402. doi:10.1007/s11095-011-0451-4
- Wu, J. W., Breydo, L., Isas, J. M., Lee, J., Kuznetsov, Y. G., Langen, R., & Glabe, C. (2010). Fibrillar oligomers nucleate the oligomerization of monomeric amyloid beta but do not seed fibril formation. *J Biol Chem*, 285(9), 6071-6079. doi:10.1074/jbc.M109.069542
- Zhang, Y., Wu, L., Gupta, P., Desai, A. A., Smith, M. D., Rabia, L. A.,... Tessier, P. M. (2020). Physicochemical Rules for Identifying Monoclonal Antibodies with Drug-like Specificity. *Mol Pharm*, 17(7), 2555-2569. doi:10.1021/acs.molpharmaceut.0c00257

FIGURES

Figure 1. **Characterization of liraglutide fibrils.** (A) Thioflavin T (ThT) fluorescence analysis of soluble and fibrillar liraglutide. (B) Atomic force microscopy (AFM) analysis of liraglutide fibrils. In (A), the excitation was performed at 444 nm, the emission spectra was collected from 475 to 550 nm, and the fluorescence spectra for the blank and soluble peptide samples overlap each other. The experiments were performed three times, and a representative example is shown. In (B), the experiments were performed once.

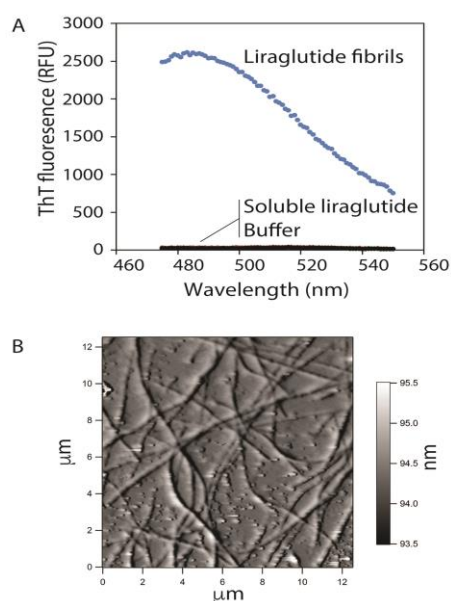


Figure 2. Evaluation of antibody purity and yield. (A) Purification yields after either one-step purification (Protein A) or two-step purification (Protein A and size-exclusion chromatography). (B) Analytical size-exclusion chromatography of select antibody variants. In (A), antibodies were expressed using suspension HEK Expi 293 cells, antibodies that were not purified using a second step purification (size-exclusion chromatography) are indicated with “*”, and the experiments were performed once. In (B), three independent experiments were performed, and the reported values are averages.

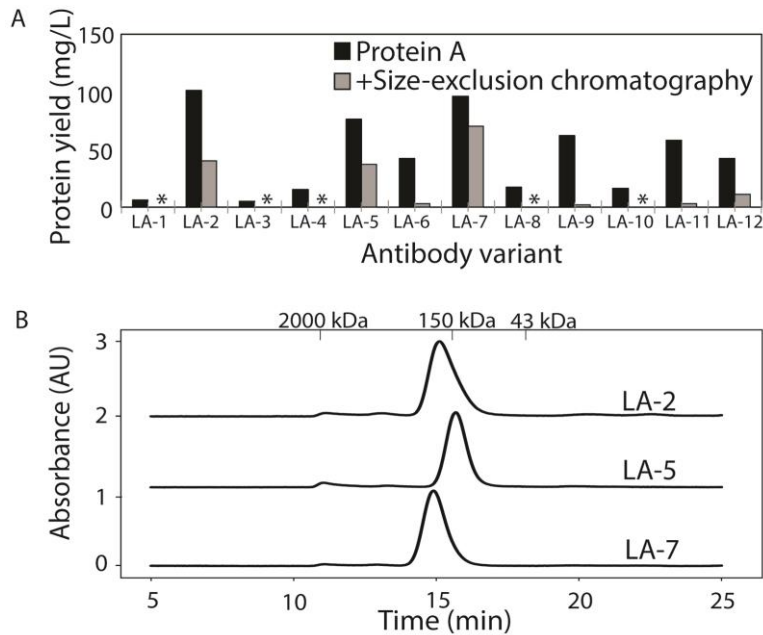


Figure 3. Initial evaluation of antibody conformational specificity for liraglutide antibodies. Antibody (5 nM) binding was evaluated to immobilized fibrillar and soluble liraglutide (10 μ M). The reported values are the raw binding signals for liraglutide fibrils divided by those for soluble liraglutide or background. The plates were pre-blocked with BSA (1 mg/mL) prior to liraglutide immobilization. Three independent experiments were performed, and the reported values are averages and the error bars are standard deviations.

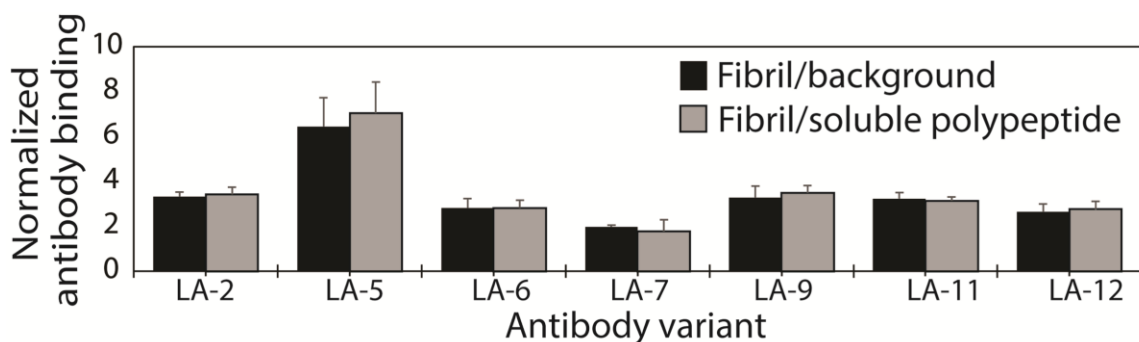


Figure 4. **Concentration-dependent binding analysis of liraglutide antibodies.**

Soluble and aggregated liraglutide samples (10 μM) were immobilized and detected at a range of antibody concentrations in PBST with 1 mg/mL BSA. The antibodies include wild type (WT), the parental clone (LA) and an affinity-matured clone (LA-5). The reported values represent raw (non-background subtracted) antibody binding signals for aggregated and soluble liraglutide. The plates were pre-blocked with BSA (1 mg/mL) prior to liraglutide immobilization. Three independent experiments were performed, and the reported values are averages and the error bars are standard deviations.

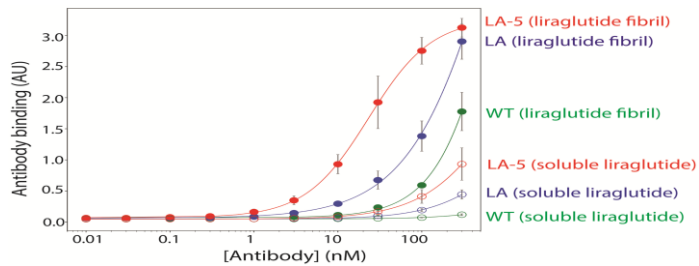


Figure 5. Evaluation of factors that impact ELISA assay sensitivity for detecting liraglutide fibrils in the presence of a large excess of soluble liraglutide. (A) Effect of BSA concentration in the antibody (LA-5) binding buffer on the detection of liraglutide fibrils. (B) Effect of antibody (LA-5) concentration on the detection of liraglutide fibrils. In (A), the antibody concentration was 100 nM. In (A) and (B), the plates were pre-blocked with BSA (1 mg/mL) prior to immobilization of liraglutide, the total peptide concentration was maintained at 1600 μM , and the reported binding signals on the y-axis are raw (non-background subtracted) signals for fibrils in the presence of soluble polypeptide divided by those for soluble polypeptide. Three independent experiments were performed, and the reported values are averages and the error bars are standard deviations.

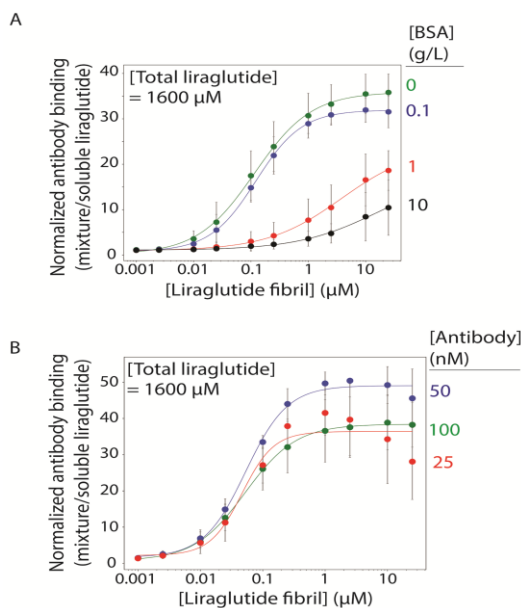


Figure 6. **Evaluation of liraglutide antibody binding to different types of amyloid fibrils.** Soluble and fibrillar peptide of liraglutide, glucagon, and α -synuclein were immobilized in ELISA plates and antibody binding was evaluated for LA-5 (50 nM). The plates were not pre-blocked with BSA prior to fibril immobilization. The reported values are background subtracted signals. Two independent experiments were performed, and the reported values are averages and the error bars are standard deviations.

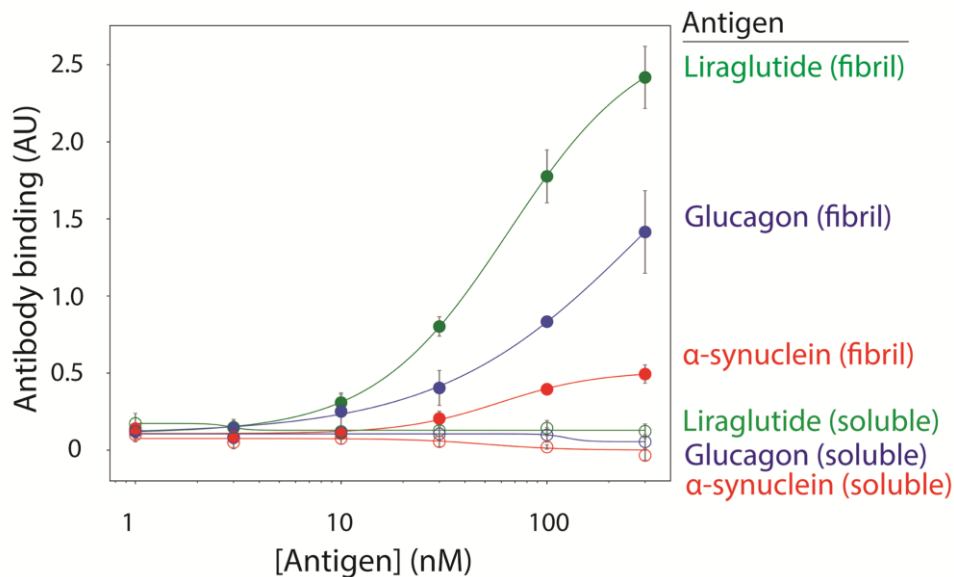


Figure 7. **Immunoblot analysis of liraglutide antibody conformational specificity.** Soluble (S) and fibrillar (F) liraglutide and glucagon samples were loaded on nitrocellulose membrane and probed with LA-5 (50 nM in PBST). A loading control blot was detected using colloidal silver stain. The experiments were repeated three times and a representative example is shown.

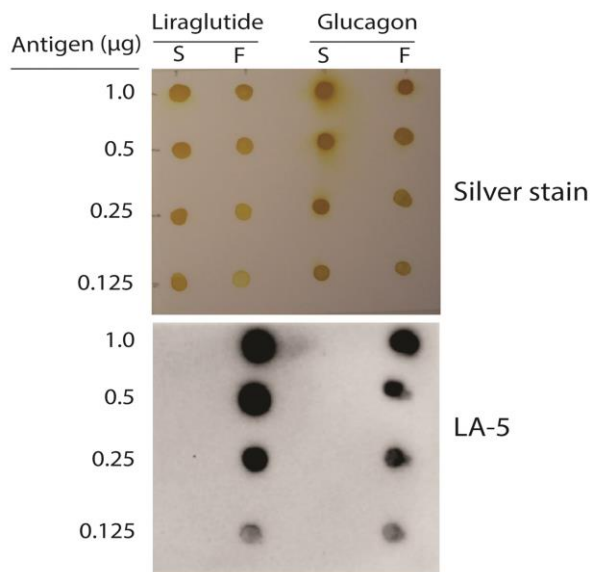


Figure 8. **Comparison of the sensitivity of ELISA and ThT assays for detecting liraglutide fibrils.** The improved ELISA assay (50 nM LA-5 antibody diluted with PBST) was compared to the ThT assay (0.4 μ M ThT, ex./em. at 444/482 nm). The total polypeptide concentration was maintained at 1600 μ M in each sample. For the ELISA assay, the plates were pre-blocked with BSA (1 mg/mL) prior to liraglutide immobilization. The reported values represent raw (non-background subtracted) signals for liraglutide fibrils in the presence of soluble polypeptide divided by those for soluble polypeptide. Four independent experiments were performed, and the reported values are averages and the error bars are standard deviations.

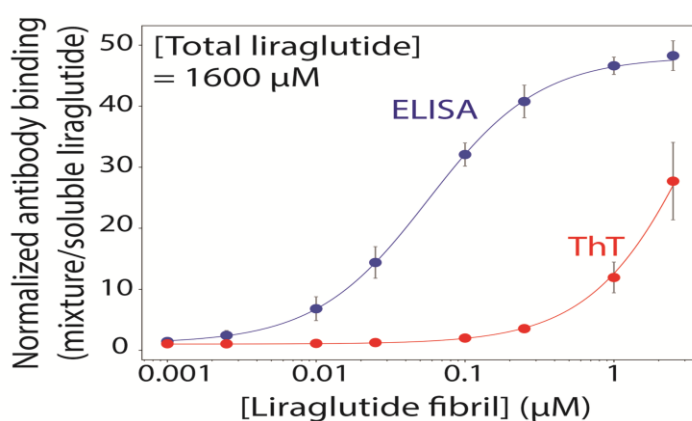


Figure 9. **Evaluation of antibody stability.** Antibody (LA-5) samples (0.1 mg/mL in PBS) were analyzed by analytical size-exclusion chromatography before and after either five freeze-thaw cycles or incubation at 25 $^{\circ}$ C for seven days. Three independent experiments were performed (two replicates per experiment), and representative examples are shown.

